Research Square

Preprints are preliminary reports that have not undergone peer review.
They should not be considered conclusive, used to inform clinical practice,
or referenced by the media as validated information.

Structural Brain Changes Across the Adult Lifespan: A Volumetric and Cortical Morphometric MRI Study

Mehmet Deniz YENER

deniz.yener@kocaeli.edu.tr

Kocaeli Üniversitesi

Halit ÇELİK

Kocaeli Üniversitesi

Özgür ÇAKIR

Kocaeli Üniversitesi

Yıldız YENER

Sakarya University

Tuncay ÇOLAK

Kocaeli Üniversitesi

Research Article

Keywords: Brain aging, Structural MRI, Brain morphometry, Cortical thickness

Posted Date: November 26th, 2026

DOI: https://doi.org/10.21203/rs.3.rs-11591064/v1

License: This work is licensed under a Creative Commons Attribution 4.0 International License.
Read Full License

Additional Declarations: No competing interests reported.

Abstract

Background

The adult human brain undergoes continuous structural remodeling, with age-related changes exhibiting marked regional heterogeneity. Quantifying these alterations across anatomical levels is fundamental for delineating physiological structural aging and for providing a reference against which pathological processes may be evaluated. This study aimed to characterize age-related structural brain alterations across the adult lifespan (21–96 years) in neurologically healthy individuals using an automated, multilevel morphometric approach, and to establish a quantitative reference framework for structural brain aging.

Methods

In this study, T1 weighted magnetic resonance images from 403 adults aged 21 to 96 years were analyzed using an automated brain mapping system. Volumetric measures of tissue components, brain regions, and cortical thickness were obtained, normalized to intracranial volume, and evaluated against age using linear regression models. Segmented regression was additionally applied to each measure to test whether age related change proceeded at a constant rate across adulthood.

Results

Increasing age was associated with reduced brain parenchymal, gray matter, and white matter volumes and increased cerebrospinal fluid volume. Volumetric decline was more pronounced in the cerebrum than the cerebellum. Among subcortical structures, the thalamus showed the strongest association with age. Cortical thickness decreased preferentially in insular, parietal, and frontal regions, with higher sensitivity observed in motor and premotor areas. Segmented analysis identified a change in the rate of volumetric decline for the whole brain, the cerebrum, cerebral white matter, the cerebellum and the hippocampus, whereas cortical thinning proceeded at an essentially constant rate throughout adulthood.

Conclusions

Structural changes accompanying brain aging show regionally differentiated patterns across tissue compartments and anatomical regions. These findings indicate that brain aging is characterized by regional differences in structural sensitivity, and in the age at which change becomes evident, rather than by a uniform process.

Background

The human brain undergoes dynamic changes across the lifespan, involving both morphological and functional alterations associated with aging [1]. In healthy adults, reductions in regional brain volumes, cortical thinning, and alterations in white matter integrity are consistently reported. These structural changes have been linked to changes with age in cognitive domains including attention, memory, and decision making [2]. Accordingly, detailed characterization of structural brain changes with age is essential not only for understanding the neurobiological features of aging but also for distinguishing patterns of healthy aging from pathological processes [3].

Volumetric changes in brain structure have important implications for brain function. Cortical thinning has been associated with declines with age in executive functions, working memory, and attentional processes [2, 3]. Similarly, hippocampal volume reduction has been regarded as a prominent neuroanatomical correlate of increased forgetfulness and learning difficulties observed with aging [4]. Alterations in white matter integrity have been linked to reductions in neuronal conduction efficiency and, consequently, to slower processing speed [2, 5]. Accordingly, quantitative characterization of volumetric changes with age in the brain and its substructures is clinically relevant for delineating the boundaries of healthy cognitive aging and for supporting the early distinction of pathological processes.

Recent advances in image processing algorithms and automated segmentation methods have enabled reliable morphometric analyses in large imaging cohorts. In particular, methods relying on multiple neural network architectures, such as AssemblyNet, support comparative analyses by improving segmentation accuracy and reproducibility [6]. By providing intracranial volume normalized volumetric measures of gray matter, white matter, CSF, lobar volumes, and subcortical nuclei, together with standardized estimates of cortical thickness derived from T1 weighted MRI images, the volBrain platform used in this study facilitates the assessment of regional neuroanatomical patterns associated with aging.

A comprehensive evaluation of the neuroanatomical signature of brain aging requires an integrated assessment that encompasses not only whole brain tissue components but also macrostructural units such as the cerebrum and cerebellum, subcortical nuclei including the thalamus and hippocampus, lobar volumes, and measures of cortical thickness. The literature indicates that rates of change with age are heterogeneously distributed across these anatomical levels, with more pronounced volumetric reduction in the frontal lobes, a more moderate and largely linear decline in the hippocampus, and lower rates of change in the striatal nuclei [7, 8]. Multilevel morphometric approaches spanning multiple anatomical scales not only support more accurate characterization of this heterogeneity but also facilitate the establishment of reference values for identifying early stages of neurodegenerative conditions [9].

In this study, morphometric changes with age were quantitatively examined in a sample spanning a broad adult age range. Using structural MRI data, tissue components, macrostructural divisions, subcortical nuclei, lobar volumes, and measures of cortical thickness were jointly analyzed in relation to age. The aim was to determine how the magnitude and rate of morphometric responses to aging vary across brain structures and to characterize whole brain and regional patterns of change associated with

healthy aging. The findings are intended to provide a quantitative reference framework for normal aging and to support comparisons with pathological patterns in future research.

Methods

Study Design and Participant Characteristics

This cross-sectional morphometric study was conducted within the fields of human neuroanatomy and neuroradiology. Structural T1 weighted brain magnetic resonance imaging data were obtained from two publicly available neuroimaging databases, the Information eXtraction from Images dataset [10] and the Open Access Series of Imaging Studies [11], both of which provide fully anonymized scans of adult participants and are widely used in neuroimaging research. The combined study sample consisted of 403 individuals aged 21 to 96 years (mean age 58.5 ± 22.7 years), including 254 women (63.0%) and 149 men (37.0%). The use of two complementary datasets aimed to increase sample size and extend age coverage across adulthood, while restricting analyses to imaging modalities and morphometric measures available in both cohorts. Participants were selected so as to provide approximately uniform coverage of each decade of adult life rather than consecutively, so that the age distribution of neither source dataset would dominate the regression estimates; the resulting composition is summarized in Table 1. For descriptive and visualization purposes, participants were stratified into decade-based age groups (20–29, 30–39, 40–49, 50–59, 60–69, 70–79, 80–89 and ≥ 90 years), whereas all statistical analyses modeled age as a continuous variable.

Table 1
Characteristics of the study sample by source dataset

Characteristic	All participants (n = 403)	IXI (n = 89)	OASIS (n = 314)
Age, years, mean (SD)	58.5 (22.7)	42.9 (10.8)	62.9 (23.3)
Age, years, range	21–96	30–68	21–96
Female, n (%)	254 (63.0)	45 (50.6)	209 (66.6)
Male, n (%)	149 (37.0)	44 (49.4)	105 (33.4)
Age group 20–29, n	48	0	48
Age group 30–39, n	57	41	16
Age group 40–49, n	50	25	25
Age group 50–59, n	50	15	35
Age group 60–69, n	50	8	42
Age group 70–79, n	50	0	50
Age group 80–89, n	50	0	50
Age group ≥ 90, n	48	0	48

Inclusion criteria included the availability of high resolution T1 weighted MRI data, the absence of documented major neurological disorders or dementia based on the source dataset criteria, and image quality adequate for automated morphometric analysis. Scans with excessive motion artifacts, magnetic field inhomogeneities, reconstruction errors, or unreliable anatomical segmentation were excluded following automated and visual quality control. The study was conducted in accordance with the Declaration of Helsinki.

MRI Data Acquisition and Preprocessing

The T1 weighted anatomical brain magnetic resonance imaging data analyzed in this study were obtained from two publicly available neuroimaging databases, the Information eXtraction from Images dataset and the Open Access Series of Imaging Studies. These databases provide structural MRI data from adult participants and are commonly used in morphometric brain research. In the IXI cohort, T1 weighted images were acquired using 1.5 Tesla and 3 Tesla MRI systems on the Philips Gyroscan Intera and Philips Intera platforms with comparable acquisition characteristics. In the OASIS cohort, structural MRI data were obtained using a standardized 1.5 Tesla MRI system with a T1 weighted magnetization prepared rapid gradient echo sequence. Across both cohorts, all images provided whole brain coverage and spatial resolution adequate for volumetric and cortical thickness analyses. To address scanner and protocol related variability associated with the use of different MRI systems and acquisition settings, all images were processed using the same automated preprocessing pipeline implemented in volBrain. This

pipeline includes denoising, bias field correction, intensity normalization, and spatial standardization [6]. Residual differences between the two source datasets in scanner platform, field strength and acquisition site were addressed by entering the source dataset as a covariate in a sensitivity analysis (Table 3).

Table 3
Age coefficients adjusted for sex and source dataset (sensitivity analysis)

Region	β adjusted (per year)	95% CI	q (age)	q (sex)	q (dataset)
Brain	-0.2045	-0.2199 to -0.1892	< 0.001	< 0.001	0.230
Brain White Matter	-0.1132	-0.1265 to -0.0999	< 0.001	0.167	0.768
Brain Gray Matter	-0.0839	-0.0949 to -0.0728	< 0.001	0.760	0.032
Cerebro Spinal Fluid	+ 0.1977	0.1820 to 0.2135	< 0.001	0.167	0.076
Cerebrum	-0.1856	-0.1997 to -0.1715	< 0.001	< 0.001	0.273
Cerebrum White Matter	-0.0688	-0.0800 to -0.0576	< 0.001	0.015	< 0.001
Cerebrum Gray Matter	-0.1168	-0.1266 to -0.1069	< 0.001	0.001	< 0.001
Cerebellum	-0.0184	-0.0218 to -0.0151	< 0.001	< 0.001	0.205
Cerebellum White Matter	-0.0062	-0.0073 to -0.0050	< 0.001	< 0.001	< 0.001
Cerebellum Gray Matter	-0.0128	-0.0157 to -0.0099	< 0.001	< 0.001	< 0.001
Thalamus	-0.0038	-0.0041 to -0.0035	< 0.001	< 0.001	0.002
Hippocampus	-0.0010	-0.0013 to -0.0007	< 0.001	0.002	0.113
Putamen	-0.0012	-0.0015 to -0.0009	< 0.001	< 0.001	0.003
Caudate nucleus	-0.0013	-0.0015 to -0.0010	< 0.001	< 0.001	< 0.001
Frontal Lobe volume	-0.0394	-0.0431 to -0.0356	< 0.001	0.005	< 0.001

β values are regression coefficients for age obtained from models that also included sex and source dataset (IXI or OASIS) as covariates, expressed as %ICV per year for volumetric measures and mm per year for cortical thickness. q values are p values adjusted for multiple comparisons using the Benjamini-Hochberg false discovery rate procedure and are reported separately for the age, sex and dataset terms.

Region	β adjusted (per year)	95% CI	q (age)	q (sex)	q (dataset)
Temporal Lobe volume	-0.0231	-0.0257 to -0.0205	< 0.001	0.427	< 0.001
Parietal Lobe volume	-0.0227	-0.0249 to -0.0205	< 0.001	< 0.001	< 0.001
Occipital Lobe volume	-0.0089	-0.0107 to -0.0072	< 0.001	0.297	< 0.001
Limbic Cortex volume	-0.0071	-0.0082 to -0.0060	< 0.001	0.015	< 0.001
Insular Cortex volume	-0.0070	-0.0077 to -0.0062	< 0.001	0.055	< 0.001
Frontal Lobe thickness (mm)	-0.0100	-0.0114 to -0.0086	< 0.001	0.092	< 0.001
Temporal Lobe thickness (mm)	-0.0072	-0.0086 to -0.0058	< 0.001	0.144	< 0.001
Parietal Lobe thickness (mm)	-0.0099	-0.0112 to -0.0086	< 0.001	0.035	< 0.001
Occipital Lobe thickness (mm)	-0.0067	-0.0080 to -0.0053	< 0.001	0.625	< 0.001
Limbic Cortex thickness (mm)	-0.0100	-0.0116 to -0.0083	< 0.001	0.002	< 0.001
Insular Cortex thickness (mm)	-0.0165	-0.0182 to -0.0148	< 0.001	0.001	< 0.001
Frontal pole thickness (mm)	-0.0098	-0.0118 to -0.0078	< 0.001	0.055	< 0.001
Middle frontal gyrus thickness (mm)	-0.0106	-0.0124 to -0.0089	< 0.001	0.069	< 0.001
Precentral gyrus thickness (mm)	-0.0114	-0.0124 to -0.0103	< 0.001	0.218	< 0.001
Superior frontal gyrus thickness (mm)	-0.0114	-0.0129 to -0.0099	< 0.001	0.427	< 0.001
Supplementary motor cortex thickness (mm)	-0.0153	-0.0170 to -0.0135	< 0.001	0.050	< 0.001

β values are regression coefficients for age obtained from models that also included sex and source dataset (IXI or OASIS) as covariates, expressed as %ICV per year for volumetric measures and mm per year for cortical thickness. q values are p values adjusted for multiple comparisons using the Benjamini-Hochberg false discovery rate procedure and are reported separately for the age, sex and dataset terms.

Image Processing and Volumetric Analysis

All morphometric analyses of T1 weighted magnetic resonance imaging data were performed using the volBrain automated brain analysis system [12]. A standardized preprocessing pipeline was applied uniformly to all images and included denoising, correction for magnetic field inhomogeneities, intensity normalization, and spatial registration to the Montreal Neurological Institute (MNI) reference space. These steps were implemented to ensure consistency of image intensity and spatial alignment across datasets acquired under different imaging conditions [6].

Following preprocessing, automated extraction of the intracranial cavity was performed, and tissue classification algorithms were applied to generate gray matter, white matter, and CSF segmentations, (Fig. 1). Volumetric measures derived from these tissue compartments were subsequently normalized to intracranial volume to account for interindividual differences in head size. Cortical morphometric analyses were conducted within the same processing framework using the AssemblyNet based cortical morphometry module, which performs automated cortical surface reconstruction and computes mean cortical thickness values, expressed in millimeters, at both lobar and region specific anatomical levels [6].

Segmentation quality was assessed using the automated quality control metrics provided by volBrain, including measures of tissue classification confidence, spatial consistency indices, and color-coded quality control outputs. In addition, all segmentations were independently reviewed by two investigators to identify cases with substantial anatomical inconsistencies or unreliable segmentation results, which were excluded from subsequent analyses. Following this review, datasets with anatomically implausible morphometric estimates, defined as mean cortical thickness below 1.2 mm across all cortical lobes, were excluded, as were observations above 96 years of age in order to limit the influence of isolated extreme values at the upper end of the age distribution on the regression estimates. The final analytic sample comprised 403 participants aged 21 to 96 years.

Statistical Methods and Analysis

All statistical analyses were performed using IBM SPSS Statistics for Windows, version 25.0 (SPSS; IBM Corp., Armonk, NY, USA). Volumetric analyses were based on measures normalized to total intracranial volume (ICV) and expressed as percentages of intracranial volume (%ICV), whereas cortical analyses used absolute mean cortical thickness (CT) values expressed in millimeters (mm).

Associations between age and morphometric measures were examined using linear regression models (LRMs), with age specified as a continuous independent variable. Linear models were used to estimate average age-associated rates of change, allowing direct comparison of regression coefficients and effect sizes across tissue compartments, macrostructural divisions, subcortical nuclei, and cortical regions. This approach was chosen to provide summary estimates of annual change rather than to characterize non-linear aging trajectories. For each LRM, we estimated and reported the unstandardized

regression coefficient (β) with its 95% confidence interval, the coefficient of determination (R^2), the p value, and Cohen's f^2 effect size. Cohen's f^2 was calculated from R^2 using standard formulas. Regression coefficients were interpreted as annual rates of change, expressed as %ICV per year for volumetric measures and mm per year for CT. Individual scanner identifiers were not available for either source dataset, so acquisition related heterogeneity could not be modelled at the level of single scanners; instead the source dataset (IXI or OASIS), which differs in scanner platform, field strength and acquisition site, was used as a proxy for this heterogeneity and, together with sex, was entered as a covariate in a sensitivity analysis. For descriptive visualization, participants were additionally stratified into decade-based age groups, whereas all inferential analyses modeled age as a continuous variable. Model assumptions, including linearity, residual distribution, and the influence of outliers, were evaluated using standard diagnostic plots. To control for multiple regional comparisons, p values were adjusted using the false discovery rate (FDR) according to the Benjamini-Hochberg procedure, and only results that remained significant after correction were interpreted. In addition to the linear models, a two-phase segmented regression model of the form $y = \beta_0 + \beta_1 \times age + \beta_2 \times (age - \psi)_+$ was fitted to each measure in order to test whether the rate of age related change remained constant across adulthood. The breakpoint ψ was estimated by a grid search across 32 to 85 years, selecting the value that minimized the residual sum of squares. Because ψ is not identified under the null hypothesis of no slope change, statistical significance was assessed using the Davies test rather than a conventional F test, and the uncertainty of ψ was quantified by the percentile interval obtained from 400 nonparametric bootstrap resamples. Segmented and linear models were compared using the Bayesian information criterion (BIC). A breakpoint was regarded as reliable only when the Davies test was significant, the segmented model improved the BIC by more than two units, the bootstrap interval spanned 20 years or less, and the estimated breakpoint did not fall at the limit of the search range. Age related patterns were visualized using scatter plots with fitted regression lines (Figs. 2–7). All β coefficients with 95% confidence intervals, R^2 values, f^2 effect sizes, and unadjusted and FDR adjusted p values are summarized in Table 2, and the corresponding sex and dataset adjusted coefficients in Table 3. Statistical significance was defined as a two-sided p value < 0.05. Claude Opus 5 (Anthropic, San Francisco, CA, USA) was used for language editing of the manuscript. The authors reviewed and verified all content and take full responsibility for it.

Table 2
Age-associated changes per year in regional brain volumes and cortical thickness (β, 95% CI, R^2, f^2, p, FDR-adjusted q)

Region	β (per year)	95% CI	R^2	f^2	p	q (FDR)
Brain	-0.2036	-0.2183 to -0.1888	0.647	1.836	< 0.001	< 0.001
Brain White Matter	-0.1129	-0.1252 to -0.1005	0.446	0.806	< 0.001	< 0.001
Brain Gray Matter	-0.0883	-0.0986 to -0.0780	0.415	0.709	< 0.001	< 0.001
Cerebro Spinal Fluid	+ 0.2019	0.1872 to 0.2166	0.646	1.824	< 0.001	< 0.001
Cerebrum	-0.1850	-0.1984 to -0.1716	0.647	1.831	< 0.001	< 0.001
Cerebrum White Matter	-0.0905	-0.1024 to -0.0786	0.358	0.557	< 0.001	< 0.001
Cerebrum Gray Matter	-0.0945	-0.1051 to -0.0839	0.432	0.760	< 0.001	< 0.001
Cerebellum	-0.0183	-0.0215 to -0.0151	0.241	0.318	< 0.001	< 0.001
Cerebellum White Matter	-0.0088	-0.0101 to -0.0075	0.310	0.450	< 0.001	< 0.001
Cerebellum Gray Matter	-0.0098	-0.0126 to -0.0070	0.104	0.116	< 0.001	< 0.001
Thalamus	-0.0035	-0.0038 to -0.0032	0.574	1.345	< 0.001	< 0.001
Hippocampus	-0.0010	-0.0013 to -0.0008	0.130	0.150	< 0.001	< 0.001
Putamen	-0.0010	-0.0013 to -0.0007	0.088	0.097	< 0.001	< 0.001
Caudate nucleus	-0.0010	-0.0012 to -0.0007	0.109	0.122	< 0.001	< 0.001
Frontal Lobe volume	-0.0320	-0.0359 to -0.0281	0.393	0.647	< 0.001	< 0.001
Temporal Lobe volume	-0.0200	-0.0225 to -0.0174	0.370	0.587	< 0.001	< 0.001
Parietal Lobe volume	-0.0189	-0.0211 to -0.0166	0.403	0.675	< 0.001	< 0.001

Region	β (per year)	95% CI	R^2	f^2	p	q (FDR)
Occipital Lobe volume	-0.0052	-0.0071 to -0.0033	0.069	0.074	< 0.001	< 0.001
Limbic Cortex volume	-0.0055	-0.0066 to -0.0044	0.196	0.243	< 0.001	< 0.001
Insular Cortex volume	-0.0054	-0.0062 to -0.0046	0.318	0.466	< 0.001	< 0.001
Frontal Lobe thickness (mm)	-0.0057	-0.0074 to -0.0040	0.100	0.112	< 0.001	< 0.001
Temporal Lobe thickness (mm)	-0.0027	-0.0044 to -0.0010	0.023	0.024	0.002	0.002
Parietal Lobe thickness (mm)	-0.0060	-0.0076 to -0.0045	0.126	0.145	< 0.001	< 0.001
Occipital Lobe thickness (mm)	-0.0019	-0.0036 to -0.0001	0.011	0.011	0.036	0.036
Limbic Cortex thickness (mm)	-0.0048	-0.0068 to -0.0029	0.055	0.059	< 0.001	< 0.001
Insular Cortex thickness (mm)	-0.0111	-0.0132 to -0.0091	0.218	0.279	< 0.001	< 0.001
Frontal pole thickness (mm)	-0.0053	-0.0075 to -0.0032	0.057	0.060	< 0.001	< 0.001
Middle frontal gyrus thickness (mm)	-0.0073	-0.0091 to -0.0055	0.135	0.156	< 0.001	< 0.001
Precentral gyrus thickness (mm)	-0.0085	-0.0097 to -0.0072	0.315	0.460	< 0.001	< 0.001
Superior frontal gyrus thickness (mm)	-0.0079	-0.0095 to -0.0062	0.179	0.218	< 0.001	< 0.001
Supplementary motor cortex thickness (mm)	-0.0099	-0.0120 to -0.0078	0.178	0.217	< 0.001	< 0.001

Results

In measurements normalized to intracranial volume, volumetric values are expressed as percent intracranial volume (%ICV), and regression coefficients represent annual rates of change (%ICV/year). Using this framework, total brain parenchymal volume decreased with age (β = -0.2036%ICV/year, R^2 = 0.647, f^2 = 1.836, $p < 0.001$). White matter and gray matter volumes showed similar negative associations with age (white matter β = -0.1129%ICV/year, R^2 = 0.446, f^2 = 0.806; gray matter β = -0.0883%ICV/year, R^2 = 0.415, f^2 = 0.709; both $p < 0.001$). By comparison, CSF volume increased with age

(β = 0.2019%ICV/year, R^2 = 0.646, f^2 = 1.824, $p < 0.001$). The magnitude of annual change followed the order parenchyma ≈ CSF > white matter > gray matter, with a CSF increase-to-parenchymal loss ratio of approximately 0.99. (Fig. 2, Table 2).

Cerebrum and cerebellum components showed negative linear associations with age. Total cerebrum volume decreased annually by -0.1850%ICV/year, with R^2 = 0.647 and f^2 = 1.831. Cerebrum white and gray matter volumes declined at comparable rates (white matter β = -0.0905%ICV/year, R^2 = 0.358; gray matter β = -0.0945%ICV/year, R^2 = 0.432). By comparison, total cerebellar volume showed a substantially lower annual decrease (β = -0.0183%ICV/year). Cerebellar white and gray matter volumes declined by -0.0088 and − 0.0098%ICV/year, respectively (Fig. 3, Table 2).

Thalamus, hippocampus, putamen, and caudate nucleus volumes decreased with age (Fig. 4). The thalamus showed the steepest annual decline (β = -0.00351%ICV/year) and the largest proportion of variance explained (R^2 = 0.574, f^2 = 1.345). Hippocampal volume declined at a rate of − 0.00105%ICV/year, whereas the volumes of the putamen and caudate nucleus declined at comparable rates of approximately − 0.00096%ICV/year. The magnitude of volume loss with age followed the order thalamus > hippocampus > putamen ≈ caudate (Table 2).

All cortical lobar volumes decreased with age (Fig. 5). The frontal lobe showed the steepest age associated slope (-0.0320%ICV per year), while temporal (-0.0200%ICV per year) and parietal (-0.0189%ICV per year) lobes exhibited comparable volume changes, with higher age associated variance observed in the parietal lobe (R^2 = 0.403). Changes with age were markedly smaller and of comparable magnitude in the limbic (-0.0055%ICV/year), insular (-0.0054%ICV/year), and occipital (-0.0052%ICV/year) cortices, although the proportion of variance explained by age differed among them (insular R^2 = 0.318, limbic R^2 = 0.196, occipital R^2 = 0.069) (Table 2). The hierarchy of volumetric change followed the order frontal > temporal ≈ parietal > limbic ≈ insular ≈ occipital.

Mean cortical thickness decreased with age across all cortical lobes. The most pronounced annual thinning was observed in the insular cortex (β = -0.0111 mm/year). Parietal (-0.0060 mm/year) and frontal (-0.0057 mm/year) lobes showed comparable thinning rates. Thinning was more limited in the limbic (-0.0048 mm/year), temporal (-0.0027 mm/year), and occipital (-0.0019 mm/year) lobes. Thickness change rates followed the order insular > parietal ≈ frontal > limbic > temporal > occipital (Fig. 6, Table 2).

Mean cortical thickness decreased with age across all frontal lobe subregions (Fig. 7). The highest annual thinning was observed in the supplementary motor cortex (β = -0.00990 mm/year), followed by the precentral gyrus (β = -0.00846 mm/year) and the superior frontal gyrus (β = -0.00786 mm/year). Thinning rates were − 0.00731 mm/year in the middle frontal gyrus and − 0.00572 mm/year for the frontal lobe as a whole, whereas the frontal pole showed the lowest rate (β = -0.00533 mm/year). Among these subregions the precentral gyrus showed the largest proportion of variance explained by age (R^2 = 0.315). The hierarchy of thickness change followed the order supplementary motor > precentral > superior frontal > middle frontal > frontal total > frontal pole (Table 2).

Segmented regression was applied to all 31 morphometric measures in order to determine whether age related change proceeded at a constant rate across adulthood. A reliable breakpoint was identified for five volumetric measures. Cerebral white matter volume increased up to 37 years (95% CI 32–40) and declined thereafter, with the slope changing from + 0.2254 to − 0.1416%ICV/year. Hippocampal volume remained stable until 50 years (95% CI 46–57) before declining (+ 0.0014 to − 0.0024%ICV/year), and cerebellar volume followed the same pattern with a breakpoint at 55 years (95% CI 50–61; +0.0047 to − 0.0371%ICV/year). Total brain parenchymal volume declined slowly until 54 years (95% CI 41–55) and approximately four times faster thereafter (− 0.0792 to − 0.2975%ICV/year), with a corresponding breakpoint at 53 years for cerebrum volume (95% CI 39–55; −0.0810 to − 0.2577%ICV/year). All five breakpoints were significant on the Davies test ($p < 0.001$). For the remaining measures, including every cortical thickness measure, no reliable breakpoint was identified; the estimated breakpoints clustered at the limits of the search range and the bootstrap intervals for the cortical thickness measures spanned 52.6 years on average, indicating that age related change in these structures is adequately described by a single constant rate.

In a sensitivity analysis in which sex and source dataset were entered as covariates, the direction of every age related association was unchanged and all 31 measures remained significant after FDR correction (Table 3). Adjustment had little influence on whole brain and macrostructural volumes (brain parenchymal volume − 0.2036 to − 0.2045%ICV/year; cerebrum − 0.1850 to − 0.1856%ICV/year), whereas cortical thickness coefficients increased in magnitude, in several regions substantially (occipital lobe thickness − 0.0019 to − 0.0067 mm/year; temporal lobe thickness − 0.0027 to − 0.0072 mm/year; limbic cortex thickness − 0.0048 to − 0.0100 mm/year). Sex contributed independently to 17 of the 31 measures and source dataset to 25, the latter affecting cortical thickness measures in particular. The unadjusted cortical thickness slopes reported above are therefore conservative rather than inflated.

[Table 2 should appear here]

[Table 3 should appear here]

Discussion

In this study, morphometric changes with age in adults without known neurological disease were evaluated across tissue compartments and major brain divisions. Reductions in gray and white matter volumes occurred alongside a concurrent increase in CSF volume, indicating that parenchymal loss and CSF expansion represent complementary components of the morphometric aging process. This pattern is consistent with prior tissue segmentation studies reporting age related decreases in total gray matter volume and a heterogeneous distribution of structural changes across the brain in healthy adults [13, 14], and with studies in which age related brain volume reductions across adulthood were accompanied by enlargement of CSF spaces [2]. The higher proportion of variance explained by age for CSF volume, compared with gray and white matter volumes, suggests that CSF expansion is more tightly associated with chronological aging, whereas parenchymal volume changes show greater heterogeneity [1, 13]. The

comparable magnitude of the gray and white matter slopes observed here is in turn consistent with models describing coordinated age related alterations affecting both cortical tissue and white matter organization [5].

Macrostructural analyses indicated differing rates of age related volume change between the cerebrum and the cerebellum. A steeper annual decline was observed for total cerebrum volume, whereas cerebellar volume showed a more gradual pattern, suggesting that age sensitivity differs between supratentorial and infratentorial structures. This dissociation is consistent with previous MRI studies showing that age related volumetric changes follow distinct patterns in the cerebrum and cerebellum and that volume loss is earlier and more pronounced in supratentorial regions [1, 3, 15], and it aligns with the differential aging framework, which emphasizes region specific sensitivity to aging across brain structures [3]. Longitudinal findings further indicate that cerebellar volume trajectories do not follow a uniform course across the lifespan [23]. Taken together, these observations support a morphometric aging profile in which supratentorial regions show greater and earlier involvement, whereas infratentorial structures exhibit a slower and more variable pattern of change.

Age related volume reductions were observed across the thalamus, hippocampus, putamen, and caudate nucleus, with clear differences in both rates of change and the proportion of variance explained by age. Among subcortical nuclei, the thalamus showed the strongest association with age, consistent with prior neuroimaging studies reporting pronounced thalamic volume loss that is not uniform and may be more marked in subdivisions with dense frontal connectivity [16]. More broadly, age related volume decline has been shown to involve multiple subcortical structures, including the thalamus and basal ganglia, in healthy adults [17, 24]. The shallower associations observed for the hippocampus suggest a more gradual pattern of volumetric change, although evidence synthesized within the differential aging framework indicates that hippocampal volume reduction can be observed across adult life while the magnitude and inter individual variability of age effects differ across subcortical structures [3]. The smaller associations detected in the putamen and caudate nucleus indicate more limited age related volumetric differences in striatal structures, consistent with reports of age related shrinkage in these nuclei [25]. The uniform age range and consistent analytical approach employed here allow a direct comparison of age sensitivity profiles across these nuclei.

Lobar volume analyses indicate that age related cortical changes are not uniformly distributed across the cortex but follow a distinct anteroposterior sensitivity gradient. Within a uniform normalization and analytical framework, the most pronounced volume reduction was observed in the frontal lobe, with more moderate changes in the temporal and parietal lobes and comparatively limited differences in the limbic, insular, and occipital cortices. This distribution is consistent with previous comparative studies reporting stronger and more consistent associations between age and frontal and parietal cortical volumes, with more limited volumetric changes in the occipital cortex [2, 3, 18]. Lifespan MRI studies have shown that cortical volume changes exhibit distinct statistical patterns across brain regions, reflecting regional heterogeneity in morphometric aging [1], and large scale population based analyses have demonstrated broader interindividual variability in frontal and temporal cortical volumes across

adulthood [9]. The combined reporting of intracranial volume normalized regression slopes and proportions of variance explained allows a direct and comparable assessment of both the magnitude and the consistency of these regional changes.

Analyses of cortical thickness indicate that age related morphometric changes are not limited to volumetric measures but can also be characterized using distinct structural metrics. Previous work has shown that cortical thickness, surface area, and gray matter volume may exhibit different regional distributions during aging, supporting the concept of cortical aging as a multidimensional morphometric process [26], and that age related cortical thinning varies across regions in both slope and magnitude [19, 20]. In the present study, thinning was most pronounced in the insular, parietal, and frontal cortices and more limited in the temporal and occipital regions, consistent with previous reports of stronger age related morphometric associations in association cortices than in posterior cortical regions [27]. In limbic predominant cortical areas the more moderate thinning suggests greater interindividual variability, in line with studies reporting heterogeneous and non-uniform lifespan trajectories of cortical thinning in the limbic cortex [9, 28]. Taken together, the combined evaluation of lobar volume and cortical thickness supports regionally differentiated morphometric patterns that are not captured by volumetric measures alone.

The frontal cortex has been consistently highlighted in the neuroimaging literature as showing increased sensitivity to morphometric changes with age within the framework of differential aging [2, 3]. In the present study, the combined evaluation of frontal subcomponents indicates that age related cortical thinning is not uniformly distributed within the frontal cortex but differs across motor and premotor systems, dorsolateral prefrontal regions, and the frontal pole. More pronounced thinning in the supplementary motor cortex and the precentral gyrus suggests greater structural sensitivity of motor and premotor areas, consistent with previous findings linking age related declines in motor performance to structural changes in medial and dorsal motor cortical regions [21, 22]. By contrast, the more moderate thinning observed in dorsolateral prefrontal regions is consistent with theoretical frameworks proposing heterogeneous expression of age related structural effects across the prefrontal cortex [3, 29], while the lower degree of thinning in the frontal pole aligns with reports describing reduced age sensitivity in this region compared with other frontal components [20]. The gradient extending from motor and premotor areas through dorsolateral prefrontal regions to the frontopolar cortex suggests that frontal cortical aging follows a functionally organized, layered pattern that parallels the intrinsic organization of the lobe rather than a single uniform vulnerability profile.

The linear models summarize the average rate of change across adulthood, whereas the segmented analysis addresses whether that rate remains constant, and the two approaches yielded different answers depending on the structure examined. Cerebral white matter volume increased until the late thirties before declining, a pattern consistent with the protracted myelination of cerebral white matter into the fourth decade and with its subsequent degeneration [1, 5]. Hippocampal and cerebellar volumes remained essentially stable until the sixth decade and declined thereafter, in line with observations that hippocampal and cerebellar trajectories are not uniform across the lifespan [8, 23]. Total brain and

cerebrum volumes showed an acceleration of loss after the mid fifties, consistent with lifespan analyses describing a non-constant rate of parenchymal decline [1]. By contrast, no reliable breakpoint was identified for any cortical thickness measure, indicating that cortical thinning proceeds at an essentially constant rate from early adulthood onward, in agreement with previous descriptions of cortical thinning across adult life [19, 20]. Taken together, these observations suggest that brain regions differ not only in the magnitude of age related change but also in the age at which that change becomes apparent, and that volumetric and cortical thickness measures capture temporally distinct components of the aging process. Because the present design is cross-sectional, an estimated breakpoint should be interpreted as the age at which the population level trend changes rather than as an event occurring within individuals.

Two features of the present sample require explicit consideration. The two source datasets differ in scanner platform, field strength and acquisition site, and they also cover different portions of the adult age range, so that dataset membership is partly confounded with age. When source dataset and sex were entered as covariates, no age related association changed direction and all remained significant after correction, while the cortical thickness coefficients became larger rather than smaller, indicating that the pooled unadjusted estimates understate rather than overstate cortical thinning. Sex contributed independently to just over half of the measures, most consistently in the thalamus, the cerebellum and the striatal nuclei, in keeping with reports of sex differences in subcortical volumes [24]. These observations support the regional pattern described above, while indicating that the absolute rates reported here should be interpreted with the composition of the sample in mind.

The findings of this study indicate that morphometric changes with age in healthy adults are not uniformly distributed across the brain but instead display a differentiated pattern across distinct anatomical levels. The combined evaluation of tissue components, subcortical nuclei, and frontal cortical subsegments indicates that sensitivity to age varies across brain regions, with more pronounced effects in some areas and more limited changes in others. Regional analyses further suggest that structural changes with age do not represent a unidirectional or homogeneous process but instead display a distribution shaped by the brain’s anatomical organization and regional characteristics. In this context, the higher sensitivity to age observed in specific cortical and subcortical regions indicates that the structural remodeling accompanying aging should be considered not as a uniform process across the brain but as one shaped by regional selectivity and distinct sensitivity profiles.

Despite the wide age range included, larger samples may enable more sensitive modeling of age associated morphometric changes, particularly at the regional level. Although volumetric measures were normalized to intracranial volume, sex and source dataset were addressed in a sensitivity analysis rather than in the primary models, and because the two source datasets cover different portions of the age range, dataset membership remains partly confounded with age. Owing to the cross-sectional design, the findings reflect age-related patterns rather than individual aging trajectories; therefore, longitudinal studies may provide complementary insights. Furthermore, despite the application of standardization procedures, scanner related heterogeneity inherent to the multicenter dataset could not be fully

eliminated. Finally, the linear models summarize average age effects and, although a segmented regression analysis was additionally performed to test for departures from a constant rate of change, more flexible non-linear approaches may characterize lifespan trajectories in greater detail.

Conclusions

This study demonstrates that structural brain changes with age in healthy adults differ significantly across distinct anatomical components and brain regions. The differentiation observed among tissue components, macrostructural divisions, subcortical nuclei, and cortical subsegments indicates that sensitivity to age is not homogeneously distributed within the brain. The combined evaluation of volumetric measures and cortical thickness change rates enables a clearer delineation of regional differences in morphological changes accompanying aging. This approach clarifies how structural changes differentiate across distinct brain components and facilitates the comparative interpretation of morphometric patterns with age. The findings provide an anatomical framework for the evaluation of structural changes characteristic of healthy aging. From a translational medicine perspective, this framework may support the development of regionally specific reference profiles for distinguishing normal aging patterns from pathological structural alterations in future clinical and research applications.

Abbreviations

BIC, Bayesian information criterion; CI, confidence interval; CSF, cerebrospinal fluid; CT, cortical thickness; FDR, false discovery rate; FRP, frontal pole; GM, grey matter; ICV, intracranial volume; IXI, Information eXtraction from Images; LRM, linear regression model; MFG, middle frontal gyrus; MNI, Montreal Neurological Institute; MPRAGE, magnetisation prepared rapid gradient echo; MRI, magnetic resonance imaging; OASIS, Open Access Series of Imaging Studies; PrG, precentral gyrus; SD, standard deviation; SFG, superior frontal gyrus; SMC, supplementary motor cortex; WM, white matter.

Declarations

Ethics approval and consent to participate

This study was approved by the Ethics Committee for Non-Invasive Clinical Research of Kocaeli University (approval number KOU-GOKAEK 2025/104) and was conducted in accordance with the Declaration of Helsinki. The study is a secondary analysis of two publicly available, fully anonymized neuroimaging datasets, the Information eXtraction from Images (IXI) dataset and the Open Access Series of Imaging Studies (OASIS). Written informed consent was obtained from all participants by the investigators of the original cohorts; no new data were acquired for the present study and the requirement for additional informed consent was therefore waived.

Consent for publication

Not applicable.

Competing interests

The authors declare that they have no competing interests.

Funding

This research received no specific grant from any funding agency in the public, commercial or not-for-profit sectors.

Author Contribution

Research idea: M.D.Y.Design of the study: M.D.Y., Ö.Ç., Y.Y.Acquisition of data for the study: H.Ç.Analysis of data for the study: M.D.Y., H.Ç., Ö.Ç.Interpretation of data for the study: M.D.Y., Ö.Ç.Drafting the manuscript: M.D.Y., Y.Y., Ö.Ç.Revising it critically for important intellectual content: T.Ç., Ö.Ç.Final approval of the version to be published: M.D.Y., Ö.Ç.

Acknowledgement

The authors thank the investigators of the Information eXtraction from Images (IXI)project and of the Open Access Series of Imaging Studies (OASIS) for making theirdata publicly available, and the developers of the volBrain platform for providingopen access to the automated segmentation pipeline. Data were provided in part byOASIS: Cross-Sectional: Principal Investigators: D. Marcus, R. Buckner,J. Csernansky, J. Morris; P50 AG05681, P01 AG03991, P01 AG026276, R01 AG021910,P20 MH071616, U24 RR021382.

Data Availability

The datasets analysed during the current study are publicly available. The IXIdataset can be accessed at https://brain-development.org/ixi-dataset/ and theOASIS dataset at https://www.oasis-brains.org/, in both cases under the data useterms specified by the respective providers. The derived morphometric datasetgenerated by the volBrain pipeline and analysed in this study is available fromthe corresponding author on reasonable request.

References

1. Coupé P, Catheline G, Lanuza E, et al. Towards a unified analysis of brain maturation and aging across the entire lifespan: a MRI analysis. Hum Brain Mapp. 2017;38:5501–18.

https://doi.org/10.1002/hbm.23743.

2. Fjell AM, Walhovd KB. Structural brain changes in aging: courses, causes and cognitive consequences. Rev Neurosci. 2010;21:187–221. https://doi.org/10.1515/revneuro.2010.21.3.187.
3. Raz N, Rodrigue KM, Kennedy KM, et al. Differential aging of the human striatum: longitudinal evidence. AJNR Am J Neuroradiol. 2003;24:1849–56.
4. Driscoll I, Davatzikos C, An Y, et al. Longitudinal pattern of regional brain volume change differentiates normal aging from MCI. Neurology. 2009;72:1906–13. https://doi.org/10.1212/WNL.0b013e3181a82634.
5. Peters A. The effects of normal aging on myelin and nerve fibers: a review. J Neurocytol. 2002;31:581–93. https://doi.org/10.1023/a:1025731309829.
6. Coupé P, Mansencal B, Clément M, et al. AssemblyNet: a large ensemble of CNNs for 3D whole brain MRI segmentation. NeuroImage. 2020;219:117026. https://doi.org/10.1016/j.neuroimage.2020.117026.
7. Farokhian F, Yang C, Beheshti I, et al. Age-related gray and white matter changes in normal adult brains. Aging Dis. 2017;8:899–909. https://doi.org/10.14336/AD.2017.0502.
8. Fraser MA, Walsh EI, Shaw ME, et al. Longitudinal trajectories of hippocampal volume in middle to older age community dwelling individuals. Neurobiol Aging. 2021;97:97–105. https://doi.org/10.1016/j.neurobiolaging.2020.10.011.
9. Bethlehem RAI, Seidlitz J, White SR, et al. Brain charts for the human lifespan. Nature. 2022;604:525–33. https://doi.org/10.1038/s41586-022-04554-y.
10. IXI – Information eXtraction from Images. Brain Development. https://brain-development.org/ixi-dataset/. Accessed 29 Oct 2026.
11. Marcus DS, Wang TH, Parker J, Csernansky JG, Morris JC, Buckner RL. Open Access Series of Imaging Studies (OASIS): cross-sectional MRI data in young, middle aged, nondemented, and demented older adults. J Cogn Neurosci. 2007;19:1498–507. https://doi.org/10.1162/jocn.2007.19.9.1498.
12. Manjón JV, Coupé P. volBrain: an online MRI brain volumetry system. Front Neuroinform. 2016;10:30. https://doi.org/10.3389/fninf.2016.00030.
13. Walhovd KB, Fjell AM, Reinvang I, et al. Effects of age on volumes of cortex, white matter and subcortical structures. Neurobiol Aging. 2005;26:1261–70. https://doi.org/10.1016/j.neurobiolaging.2005.05.020.
14. Good CD, Johnsrude IS, Ashburner J, et al. A voxel-based morphometric study of ageing in 465 normal adult human brains. NeuroImage. 2001;14:21–36. https://doi.org/10.1006/nimg.2001.0786.
15. Jernigan TL, Archibald SL, Fennema-Notestine C, et al. Effects of age on tissues and regions of the cerebrum and cerebellum. Neurobiol Aging. 2001;22:581–94. https://doi.org/10.1016/s0197-4580(01)00217-2.

16. Hughes EJ, Bond J, Svrckova P, et al. Regional changes in thalamic shape and volume with increasing age. NeuroImage. 2012;63:1134–42. https://doi.org/10.1016/j.neuroimage.2012.07.043.
17. Goodro M, Sameti M, Patenaude B, Fein G. Age effect on subcortical structures in healthy adults. Psychiatry Res. 2012;203:38–45. https://doi.org/10.1016/j.pscychresns.2011.09.014.
18. Allen JS, Damasio H, Grabowski TJ. Normal neuroanatomical variation in the human brain: an MRI-volumetric study. Am J Phys Anthropol. 2002;118:341–58. https://doi.org/10.1002/ajpa.10092.
19. Salat DH, Buckner RL, Snyder AZ, et al. Thinning of the cerebral cortex in aging. Cereb Cortex. 2004;14:721–30. https://doi.org/10.1093/cercor/bhh032.
20. Hogstrom LJ, Westlye LT, Walhovd KB, Fjell AM. The structure of the cerebral cortex across adult life: age-related patterns of surface area, thickness, and gyrification. Cereb Cortex. 2013;23:2521–30. https://doi.org/10.1093/cercor/bhs231.
21. Seidler RD, Bernard JA, Burutolu TB, et al. Motor control and aging: links to age-related brain structural, functional, and biochemical effects. Neurosci Biobehav Rev. 2010;34:721–33. https://doi.org/10.1016/j.neubiorev.2009.10.005.
22. Rosano C, Aizenstein H, Brach J, et al. Gait measures indicate underlying focal gray matter atrophy in the brain of older adults. J Gerontol Biol Sci Med Sci. 2008;63:1380–8. https://doi.org/10.1093/gerona/63.12.1380.
23. Romero JE, Coupé P, Lanuza E, et al. Toward a unified analysis of cerebellum maturation and aging across the entire lifespan: a MRI analysis. Hum Brain Mapp. 2021;42:1287–303. https://doi.org/10.1002/hbm.25293.
24. Wang Y, Xu Q, Luo J, et al. Effects of age and sex on subcortical volumes. Front Aging Neurosci. 2019;11:259. https://doi.org/10.3389/fnagi.2019.00259.
25. Abedelahi A, Hasanzadeh H, Hadizadeh H, Joghataie MT. Morphometric and volumetric study of caudate and putamen nuclei in normal individuals by MRI: effect of normal aging, gender and hemispheric differences. Pol J Radiol. 2013;78:7–14. https://doi.org/10.12659/PJR.889364.
26. Lemaitre H, Goldman AL, Sambataro F, et al. Normal age-related brain morphometric changes: nonuniformity across cortical thickness, surface area and gray matter volume? Neurobiol Aging. 2012;33:e6171–9. https://doi.org/10.1016/j.neurobiolaging.2010.07.013.
27. Fjell AM, Walhovd KB, Fennema-Notestine C, et al. One-year brain atrophy evident in healthy aging. J Neurosci. 2009;29:15223–31. https://doi.org/10.1523/JNEUROSCI.3252-09.2009.
28. Vidal-Pineiro D, Parker N, Shin J, et al. Cellular correlates of cortical thinning throughout the lifespan. Sci Rep. 2020;10:21803. https://doi.org/10.1038/s41598-020-78471-3.
29. West R. In defense of the frontal lobe hypothesis of cognitive aging. J Int Neuropsychol Soc. 2000;6:727–9. https://doi.org/10.1017/s1355617700666109.

Figures

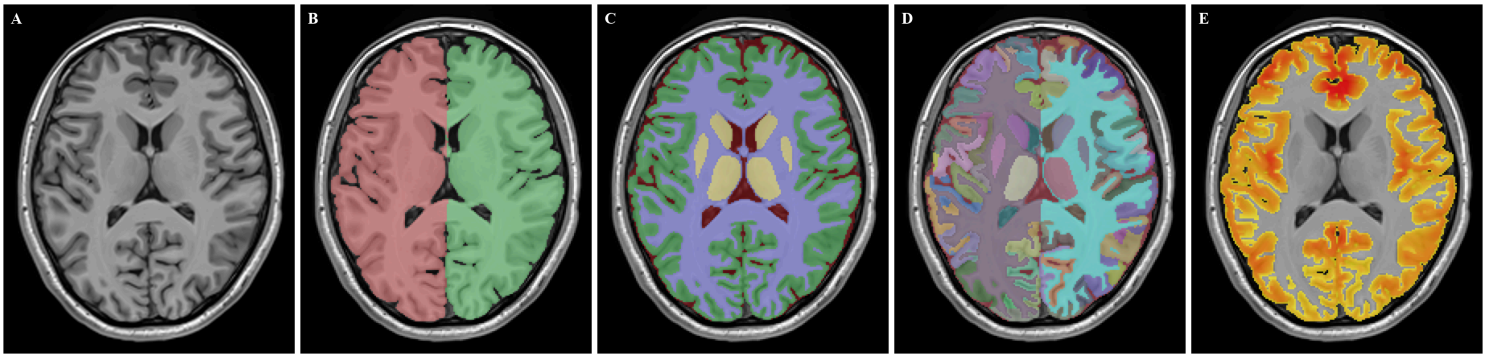

Figure 1

Automated brain segmentation and morphometric outputs of the volBrain framework. All panels show the same representative axial section. A T1-weighted magnetic resonance image. B Macrostructural segmentation. C Tissue segmentation. D Subcortical and cortical structure segmentation. E Cortical thickness map

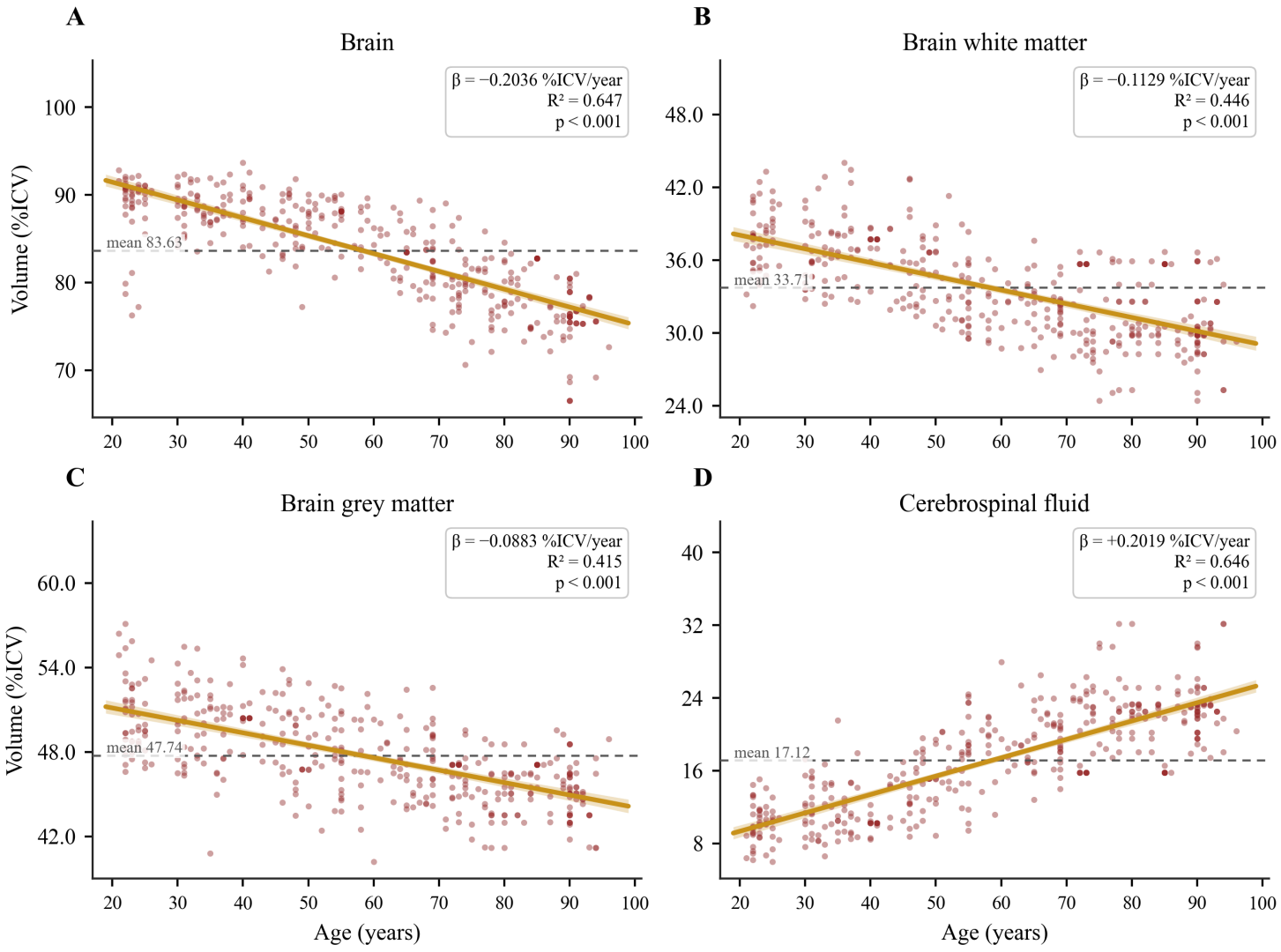

Figure 2

Changes in whole brain tissue composition across the adult lifespan. Scatter plots show individual values for all 403 participants against age in years. The solid line is the ordinary least squares regression fit, the shaded band its 95% confidence interval, and the dashed horizontal line the sample mean. A Brain. B Brain white matter. C Brain grey matter. D Cerebrospinal fluid. Volumes are expressed as percentage of intracranial volume (%ICV).

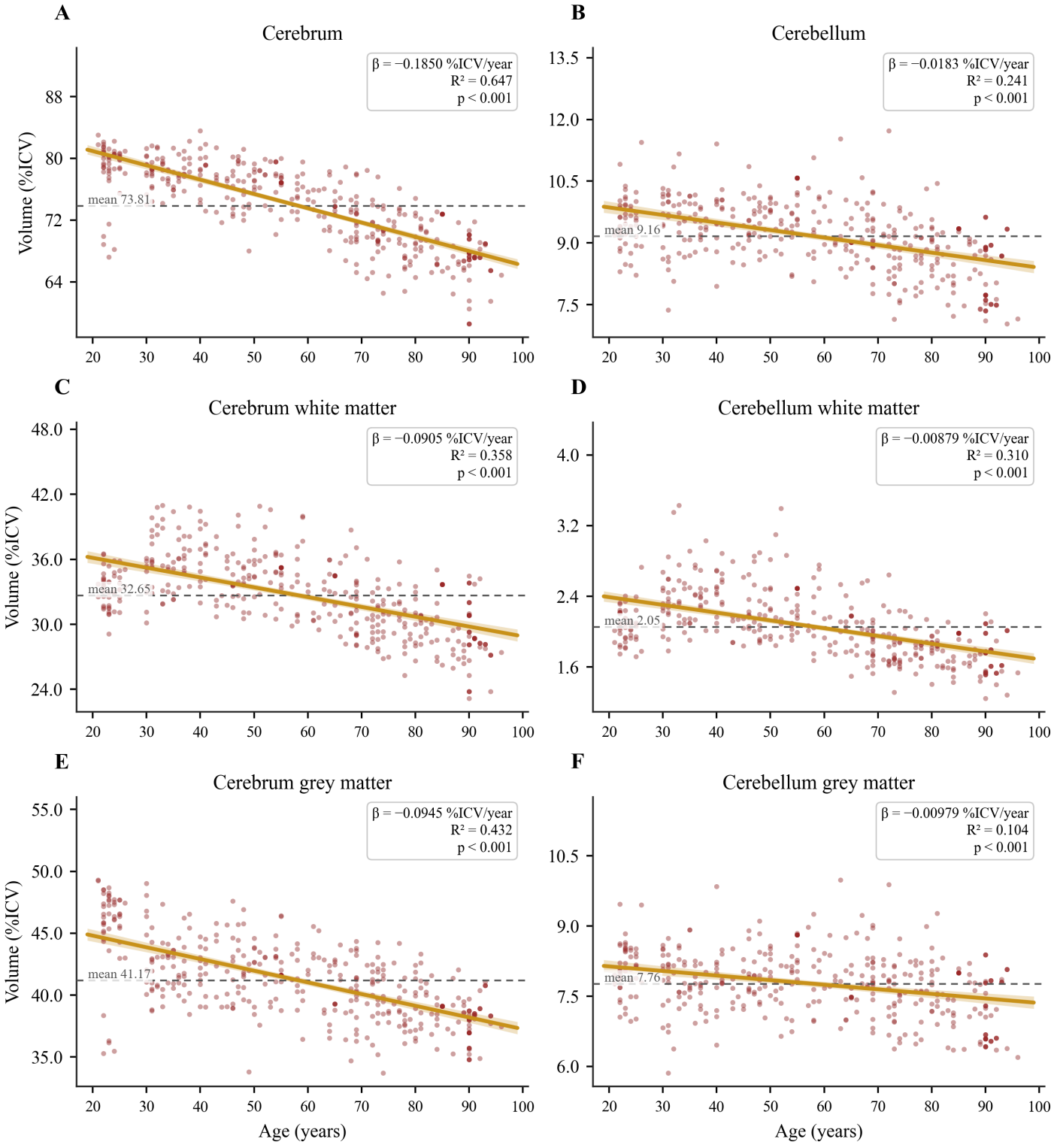

Figure 3

Macrostructural volume changes in the cerebrum and cerebellum across age. Scatter plots show individual values for all 403 participants against age in years. The solid line is the ordinary least squares regression fit, the shaded band its 95% confidence interval, and the dashed horizontal line the sample mean. A Cerebrum. B Cerebellum. C Cerebrum white matter. D Cerebellum white matter. E Cerebrum grey matter. F Cerebellum grey matter. Volumes are expressed as percentage of intracranial volume (%ICV).

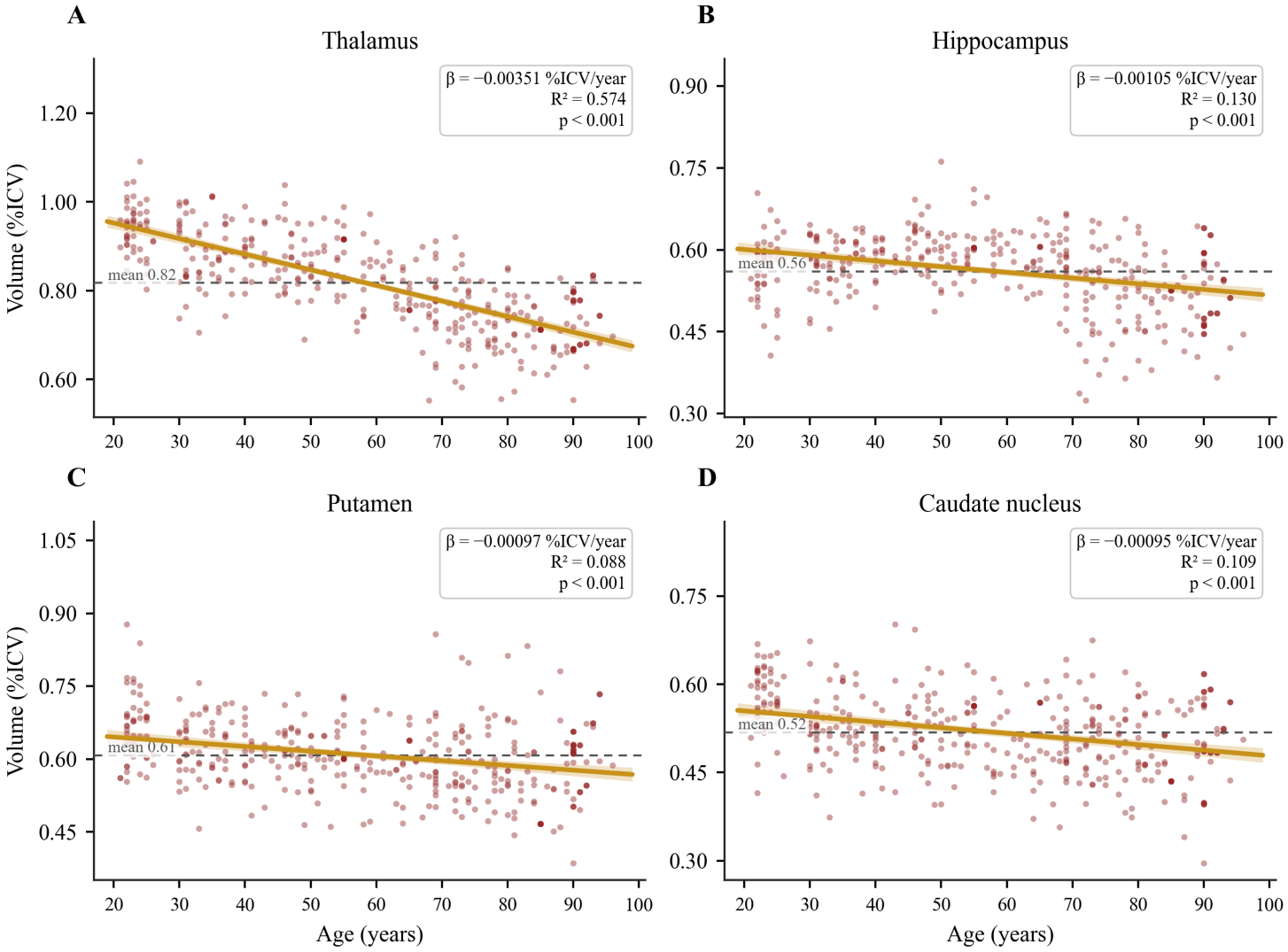

Figure 4

Volumetric patterns of age associated change in major subcortical nuclei. Scatter plots show individual values for all 403 participants against age in years. The solid line is the ordinary least squares regression fit, the shaded band its 95% confidence interval, and the dashed horizontal line the sample mean. A Thalamus. B Hippocampus. C Putamen. D Caudate nucleus. Volumes are expressed as percentage of intracranial volume (%ICV).

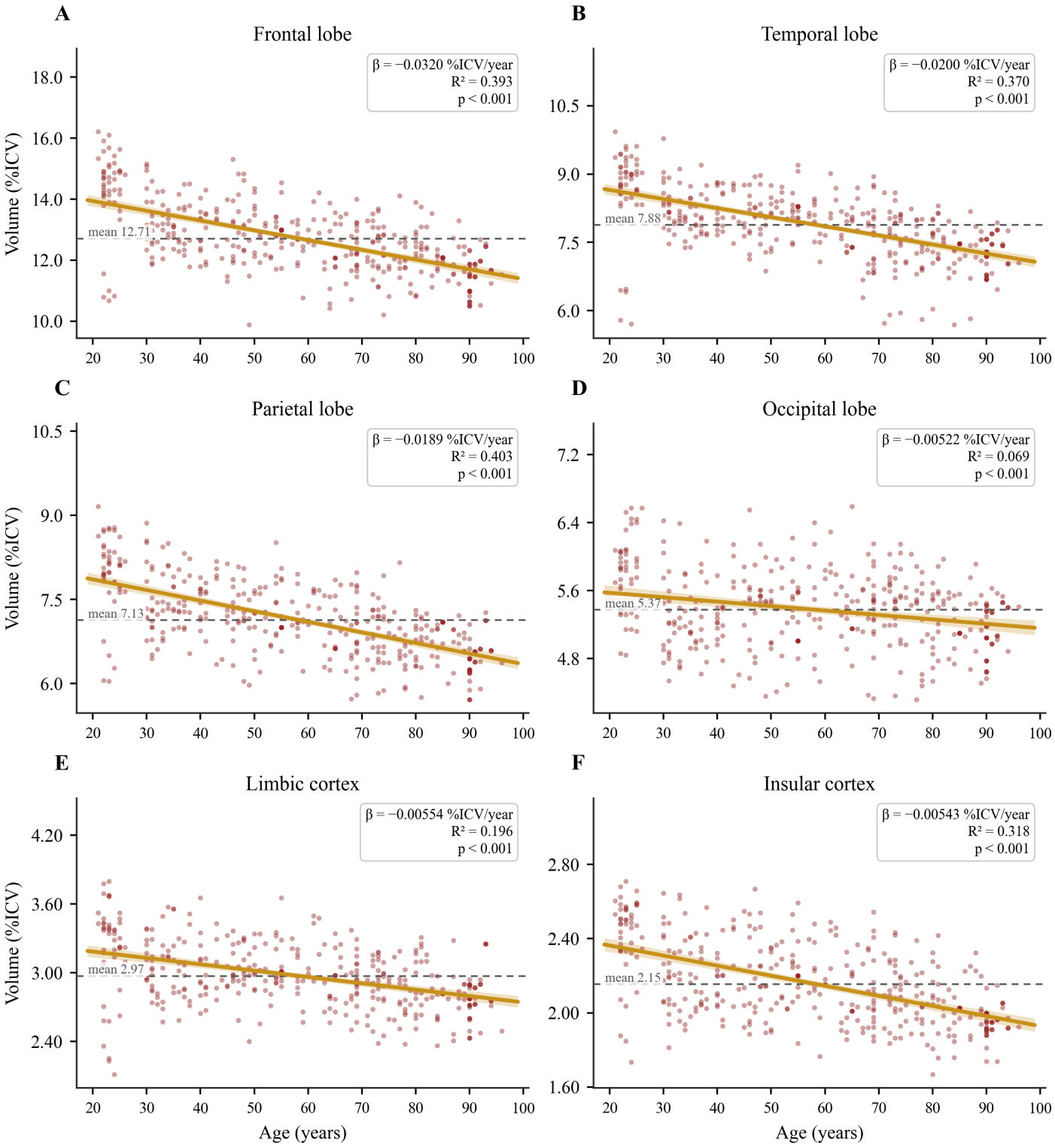

Figure 5

Lobar distribution of cortical volume changes across the adult lifespan. Scatter plots show individual values for all 403 participants against age in years. The solid line is the ordinary least squares regression fit, the shaded band its 95% confidence interval, and the dashed horizontal line the sample mean. A Frontal lobe. B Temporal lobe. C Parietal lobe. D Occipital lobe. E Limbic cortex. F Insular cortex. Volumes are expressed as percentage of intracranial volume (%ICV).

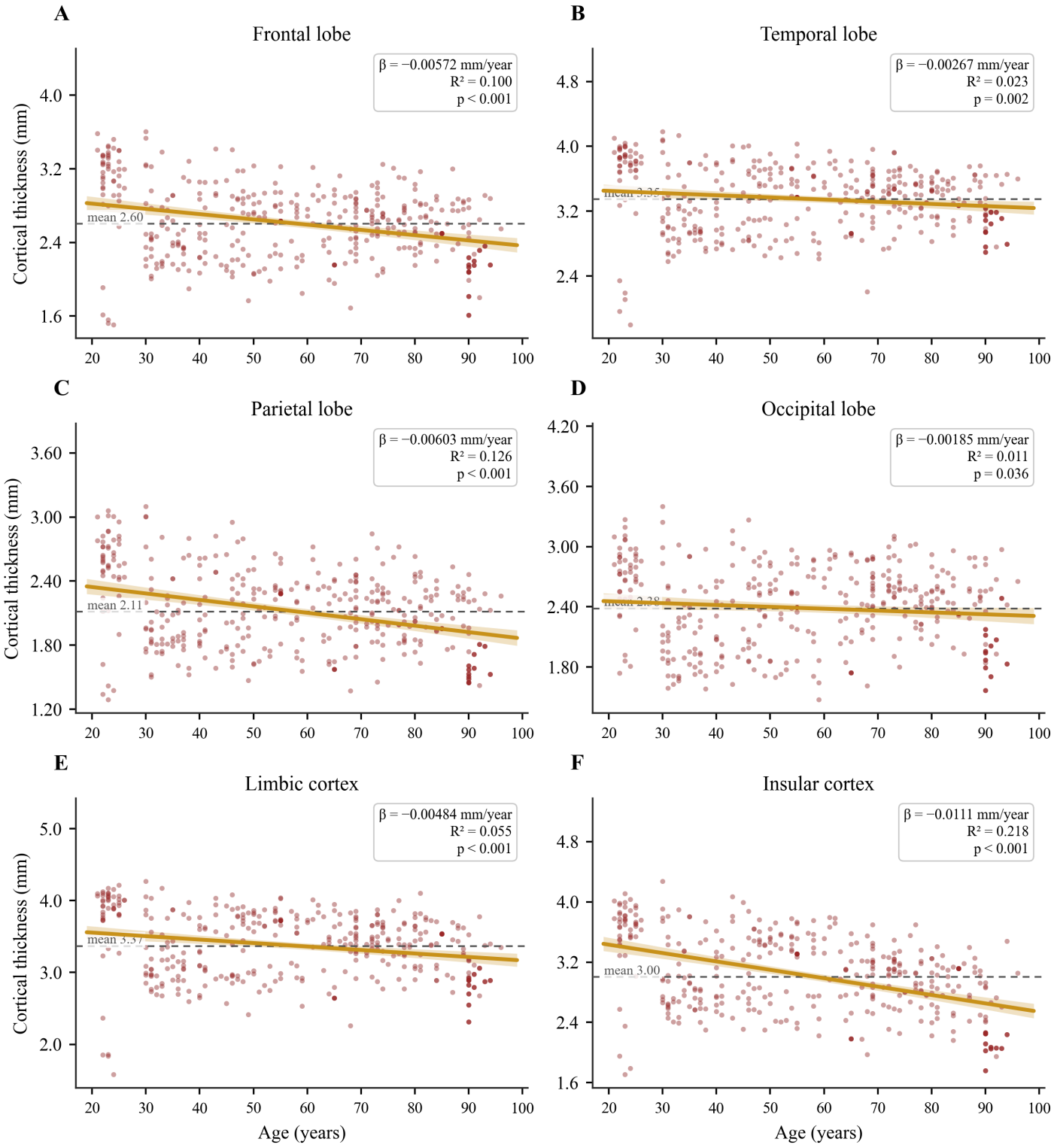

Figure 6

Lobar patterns of cortical thickness change across age. Scatter plots show individual values for all 403 participants against age in years. The solid line is the ordinary least squares regression fit, the shaded band its 95% confidence interval, and the dashed horizontal line the sample mean. A Frontal lobe. B Temporal lobe. C Parietal lobe. D Occipital lobe. E Limbic cortex. F Insular cortex. Mean cortical thickness is expressed in millimetres.

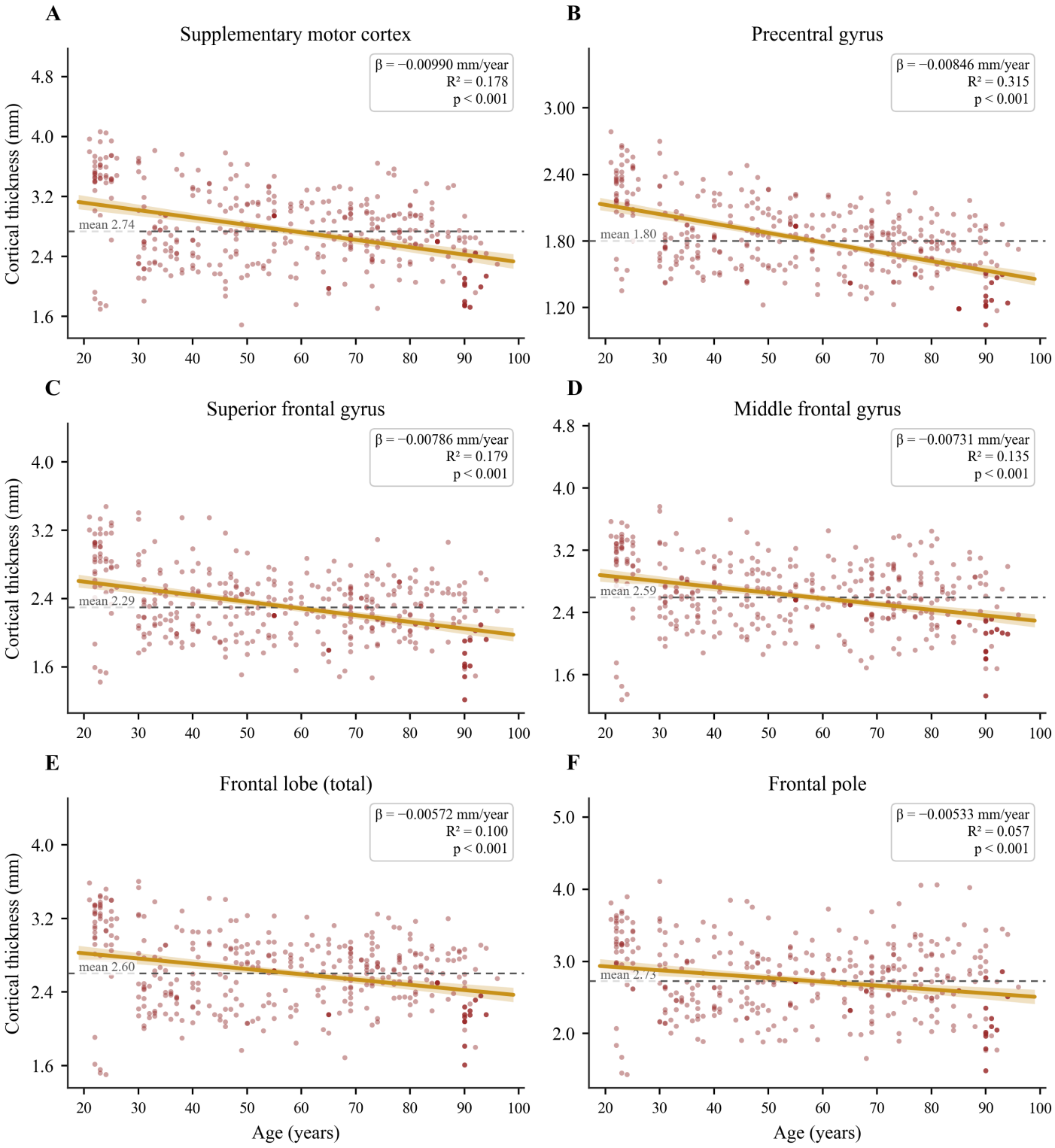

Figure 7

Cortical thickness changes within frontal lobe subregions across age. Scatter plots show individual values for all 403 participants against age in years. The solid line is the ordinary least squares regression fit, the shaded band its 95% confidence interval, and the dashed horizontal line the sample mean. A Supplementary motor cortex. B Precentral gyrus. C Superior frontal gyrus. D Middle frontal gyrus. E Frontal lobe (total). F Frontal pole. Mean cortical thickness is expressed in millimetres.